Journal of Rock Mechanics and Geotechnical Engineering 13 (2021) 1413–1427

Contents lists available at ScienceDirect

Journal of Rock Mechanics and Geotechnical Engineering

journal homepage: www.jrmge.cn

Full Length Article

Prediction of flyrock distance induced by mine blasting using a novel Harris Hawks optimization-based multi-layer perceptron neural network

Bhatawdekar Ramesh Murlidhar [a,b], Hoang Nguyen [c,d,*], Jamal Rostami [e], XuanNam Bui [c,d], Danial Jahed Armaghani [f,**], Prashanth Ragam [g], Edy Tonnizam Mohamad [a]

[a] Centre of Tropical Geoengineering (Geotropik), School of Civil Engineering, Faculty of Engineering, Universiti Teknologi Malaysia, Skudai, Johor, 81310, Malaysia
[b] Department of Mining Engineering, Indian Institute of Technology, Kharagpur, 721302, India
[c] Department of Surface Mining, Mining Faculty, Hanoi University of Mining and Geology, Hanoi, 100000, Viet Nam
[d] Innovations for Sustainable and Responsible Mining (ISRM) Group, Hanoi University of Mining and Geology, Hanoi, 100000, Viet Nam
[e] Department of Mining Engineering, Earth Mechanics Institute, Colorado School of Mines, Golden, CO, 80401, USA
[f] Department of Urban Planning, Engineering Networks and Systems, Institute of Architecture and Construction, South Ural State University, Chelyabinsk, 454080, Russia
[g] Department of ECE, Kakatiya Institute of Technology and Science, Warangal, 506015, India

ARTICLE INFO

Article history:
Received 20 May 2021
Received in revised form
16 July 2021
Accepted 18 August 2021
Available online 21 October 2021

Keywords:
Flyrock
Harris hawks optimization (HHO)
Multi-layer perceptron (MLP)
Random forest (RF)
Support vector machine (SVM)
Whale optimization algorithm (WOA)

ABSTRACT

In mining or construction projects, for exploitation of hard rock with high strength properties, blasting is frequently applied to breaking or moving them using high explosive energy. However, use of explosives may lead to the flyrock phenomenon. Flyrock can damage structures or nearby equipment in the surrounding areas and inflict harm to humans, especially workers in the working sites. Thus, prediction of flyrock is of high importance. In this investigation, examination and estimation/forecast of flyrock distance induced by blasting through the application of five artificial intelligent algorithms were carried out. One hundred and fifty-two blasting events in three open-pit granite mines in Johor, Malaysia, were monitored to collect field data. The collected data include blasting parameters and rock mass properties. Site-specific weathering index (WI), geological strength index (GSI) and rock quality designation (RQD) are rock mass properties. Multi-layer perceptron (MLP), random forest (RF), support vector machine (SVM), and hybrid models including Harris Hawks optimization-based MLP (known as HHO-MLP) and whale optimization algorithm-based MLP (known as WOA-MLP) were developed. The performance of various models was assessed through various performance indices, including a10-index, coefficient of determination (R^2), root mean squared error (RMSE), mean absolute percentage error (MAPE), variance accounted for (VAF), and root squared error (RSE). The a10-index values for MLP, RF, SVM, HHO-MLP and WOA-MLP are 0.953, 0.933, 0.937, 0.991 and 0.972, respectively. R^2 of HHO-MLP is 0.998, which achieved the best performance among all five machine learning (ML) models.

1. Introduction

Blasting is considered as a standard method for breaking or moving hard rock in most of the civil and mining engineering applications (Bhandari, 1997; Roy, 2005; Tatiya, 2005). During blasting, only a limited percentage (20%–30%) of explosive energy is used for the movement of blasting rock piles and rock fragmentation (Finn et al., 2004; Khandelwal and Singh, 2005). The remaining energy is dissipated, causing negative impacts including ground vibration, air overpressure, and flyrock (Khandelwal, 2011; Zhou et al., 2019; Nguyen et al., 2020). Of those, flyrock is considered a dangerous side effect that can be fatal (Guo et al., 2019a; Nguyen et al., 2019a).

To control flyrock distance in open-pit mines, blast design parameters, also known as controllable parameters, have been suggested. These parameters include hole diameter (d), powder factor (PF), burden (B), explosive charge per meter (CPM), and stemming

* Corresponding author. Department of Surface Mining, Mining Faculty, Hanoi University of Mining and Geology, Hanoi, 100000, Viet Nam.
** Corresponding author.
E-mail addresses: nguyenhoang@humg.edu.vn (H. Nguyen), danialarmaghani@susu.ru (D.J. Armaghani).
Peer review under responsibility of Institute of Rock and Soil Mechanics, Chinese Academy of Sciences.

https://doi.org/10.1016/j.jrmge.2021.08.005

length (*ST*) (Workman and Calder, 1994; Bhowmik et al., 2004; Monjezi et al., 2011; Rezaei et al., 2011). Indeed, Lundborg et al. (1975) recommended an empirical formula for approximating flyrock distance, and they claimed that flyrock distance depends on the hole diameter. Also, Olofsson (1990) developed an empirical formula for predicting flyrock distance, considering the ratio of stemming to burden (*ST*/*B*). Subsequently, Trivedi et al. (2014) considered another empirical formula to approximate flyrock distance using the relationship of *ST*/*B* and rock quality designation (*RQD*). Besides, many researchers also studied empirical equations for estimating flyrock distance, and most of them used the controllable parameters of blasting (Bagchi and Gupta, 1990; Richards and Moore, 2004; Little, 2007; Ghasemi et al., 2012; Armaghani et al., 2016a).

Based on a review of the previous works for the prediction of flyrock distance using artificial intelligence (AI) techniques (as summarized in Table 1), it has been identified that researchers used the controllable parameters of blasting and several uncertainty parameters of rock mass to predict flyrock distance. Most researchers used a single uncertain parameter for such prediction (Monjezi et al., 2011, 2012; Rezaei et al., 2011; Armaghani et al., 2014, 2016b; Marto et al., 2014; Raina and Murthy, 2016; Hasanipanah et al., 2017, 2018; Rad et al., 2018; Hudaverdi and Akyildiz, 2019; Lu et al., 2019a). Several computational models were also developed with controllable parameters for the prediction of flyrock distance (Armaghani et al., 2016b; Faradonbeh et al., 2016; Guo et al., 2019a; Nguyen et al., 2019a, 2020; Zhou et al., 2019; Han et al., 2020; Masir et al., 2020; Murlidhar et al., 2020). Nevertheless, weathering index (*WI*) has not been investigated in predicting flyrock distance. Therefore, this study investigates the influences of geological parameters such as geological strength index (*GSI*), *WI*, and RQD, to estimate the distance of flyrock in open-pit granite mines. The controllable parameters of blasting were also used for the same purposes, including *ST*/*B*, hole depth (*HD*), explosive *CPM*, and *PF*.

In the last few years, AI was recognized as avant-garde technique to effectively solve various problems in real life (Mellit and Kalogirou, 2008; Nourani et al., 2014; Renzi et al., 2014; Raza and Khosravi, 2015; Li et al., 2017; Liu et al., 2018; Rahmanifard and Plaksina, 2019; De Silva et al., 2020; Nguyen et al., 2019b, c, 2021; Zhang et al., 2020a, 2021a, b). For solving various geotechnical issues, many researchers have used various soft computing techniques such as ensemble learning methods (ELMs), including the extreme gradient boosting (XGBoost) and random forest regression (RFR) (Chen et al., 2020; Wang et al., 2020; Zhang et al., 2020b, 2021b, c). Numerous scholars have also developed and applied AI models to estimate flyrock distance aiming to overcome the drawbacks of empirical methods, as listed in Table 1. Nonetheless, they cannot represent all areas since the rock mass properties and explanation ability of the introduced models are different.

Therefore, this study proposed a novel hybrid AI model to estimate flyrock distance by considering the uncertainty parameters of rock mass and controllable parameters of blasting with high accuracy, i.e. the Harris Hawks optimization (HHO)-based multilayer perceptron (MLP) (HHO-MLP) neural network. Besides, another four AI models were also used to predict flyrock distance and compare with the results obtained by the HHO-MLP model. These four models include both hybrid and conventional models: Whale optimization algorithm-based MLP (WOA-MLP), MLP, support vector machine (SVM), and random forest (RF) and an empirical equation.

2. The novel HHO-MLP model for estimating flyrock distance

In the development of the MLP model, designing the structure and calculating the pertinent weights are challenging issues for engineers and researchers. It is difficult to identify the MLP model's optimal structure and weights, and the model is easily trapped in a local minimum (Yi and Ge, 2005). Whereas the HHO algorithm is introduced with an advantage that can optimize any problems

Table 1
Flyrock prediction techniques with AI algorithms.

Reference	AI algorithm	Parameter used for flyrock distance prediction	
		Controllable	Uncertain
Monjezi et al. (2010)	ANN	*HD, ST, BS, SpD, PF, C, N*	*RD*
Rezaei et al. (2011)	FIS, SM	*B, S, HD, ST, SpD, PF, C*	*RD*
Bahrami et al. (2011)	ANN	*B, S, HD, ST, PF, C*	*BI, RMR*
Monjezi et al. (2011)	ANN	*d, B, HD, ST, BS, SpD, PF, C*	*BI*
Ghasemi et al. (2012)	MVRA	*d, B, HD, ST, PF, Q*	
Monjezi et al. (2012)	ANN-GA	*B, S, HD, ST, SpD, PF, C*	*RMR*
Armaghani et al. (2014)	ANN-PSO	*d, B, S, HD, ST, SpD, PF, C, N*	*RD*
Marto et al. (2014)	ANN-ICA	*ST, HD, BS, PF, C*	*RD*
Trivedi et al. (2014)	MVRA	*B, S, CPM, Q*	σ_c, *RQD*
Trivedi et al. (2015)	ANN, ANFIS	*d, B, S, HD, Q, CPM*	σ_c, *RQD*
Armaghani et al. (2016a)	MVRA	*B, S, ST, HD, C*	*RMR*
Faradonbeh et al. (2016)	GP, GEP	*B, S, ST, HD, PF*	
Raina and Murthy (2016)	Empirical	*BDF, EDF*	*RMR*
Trivedi et al. (2016)	MVRA, BPNN	*B, S, CPM, PF*	σ_c, *RQD*
Hasanipanah et al. (2017)	PSO, MLR	*B, S, ST, PF*	*RD*
Asl et al. (2018)	ANN, FA	*B, S, HD, ST, PF, C*	*GSI*
Hasanipanah et al. (2018)	RES	*D, B, S/B, ST/B, HD, PF, C, VoD*	*BI, RMR*
Rad et al. (2018)	LS-SVM, SVR	*B/S, H/B, SpD, PF, C*	*RD*
Lu et al. (2019b)	Linear Regression	*B, S, ST, PF*	*RD*
Hudaverdi and Akyildiz (2019)	MDA	*B/d, S/B, ST/B, H/B, PF*	X_b
Hasanipanah and Amnieh (2020)	FRES	*B, S/B, ST/B, H/B, d, B/d, PF, C, VoD*	*RMR, BI*

Note: ANN - Artificial neural network; FIS - Fuzzy inference system; SM - Statistical methods; GA - Genetic algorithm; PSO - Particle swarm optimization; ICA -Imperialist competitive algorithm; MLR - Multiple linear regression; LS-SVM - Least squares-support vector machine; SVR - Support vector regression; FA - Firefly algorithm; MVRA - Multivariate regression analysis; MDA - Multiple discriminant analysis; FRES - Fuzzy rock engineering system; GEP - Gene expression programming; GP - Genetic programming; BPNN - Back propagation neural network; S - Spacing (m); HD = hole depth (m); H = Bench height (m); SpD = Specific drilling (m/m^3); C = Maximum charge per delay (kg); Q = Charge per blast hole (kg); VoD = Velocity of detonation of explosives (m/s); N = Number of rows; RD = Rock density (kg/m^3); RMR = Rock mass rating; BI = Blastability index (%); σ_c = Uniaxial compressive strength (MPa); X_b = Block size (m); BDF = Blast design factor; RMF = Rock mass factor; EDF = Explosives design factor.

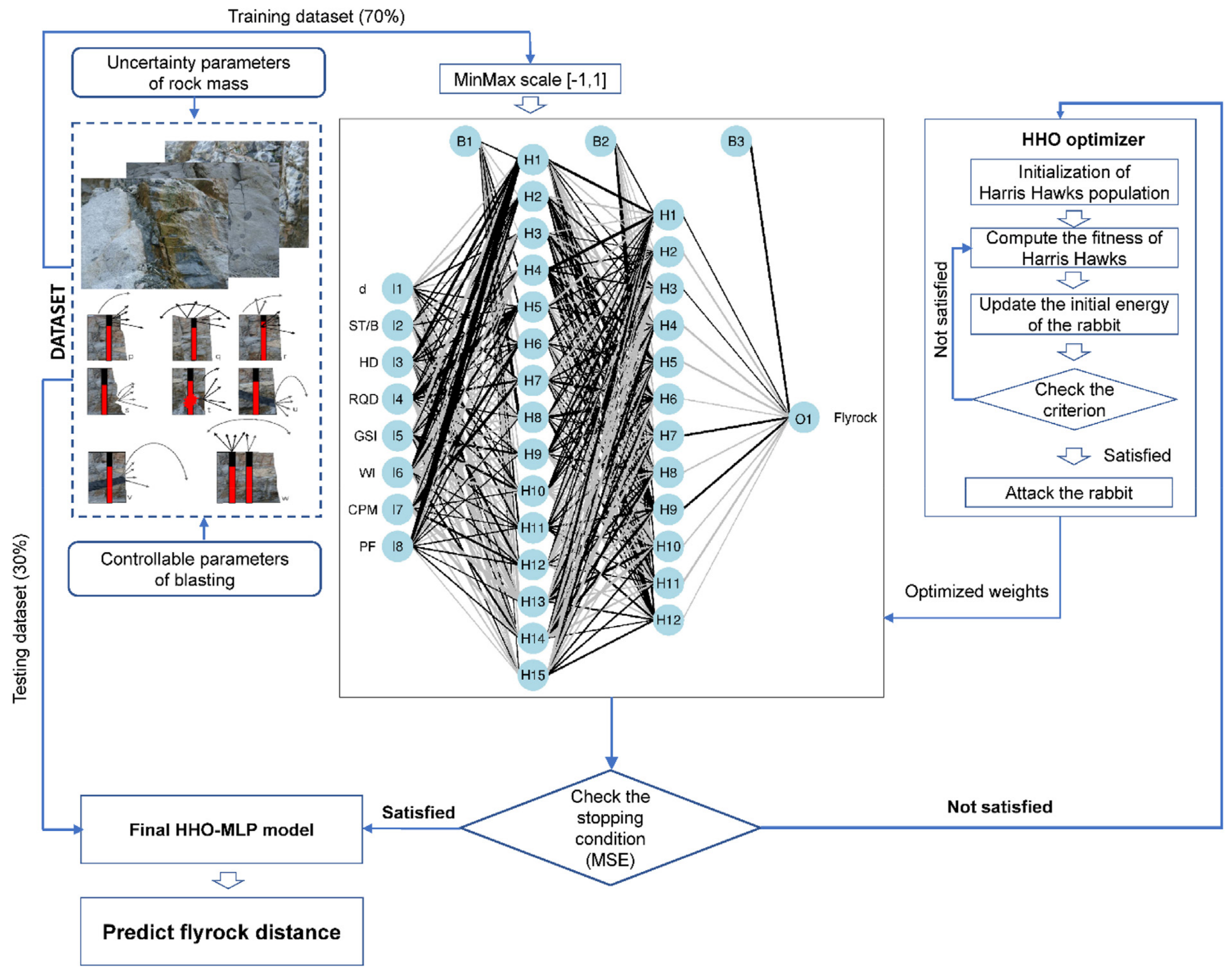

Fig. 1. The proposed novel HHO-MLP framework for predicting flyrock distance by considering rock mass properties and blasting criteria.

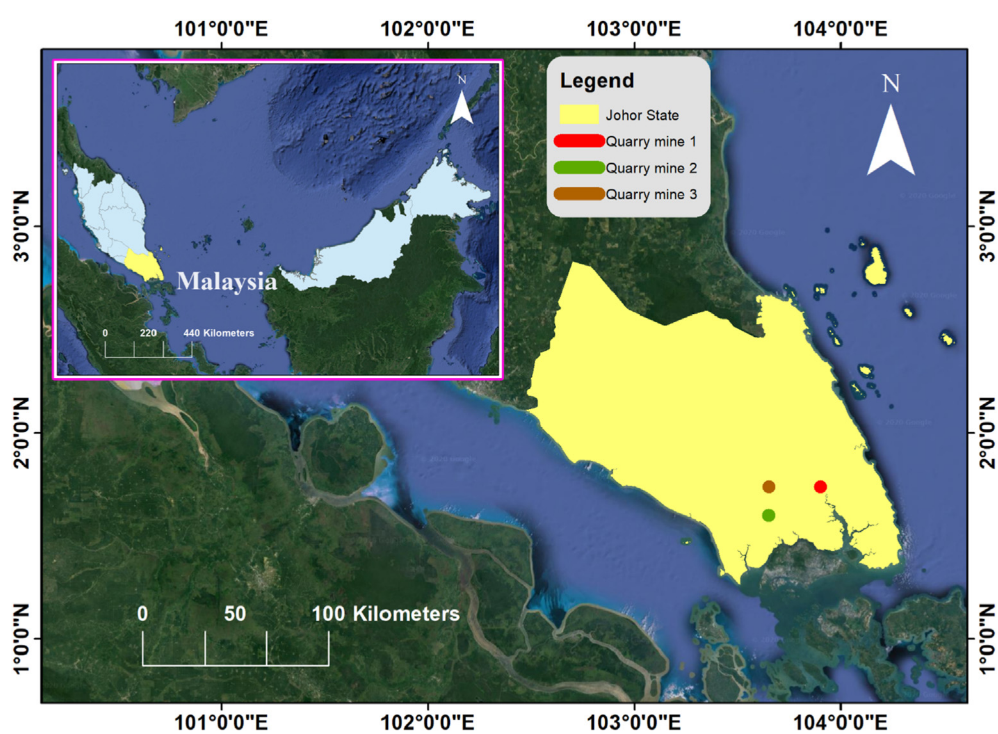

Fig. 2. Locations of three granite mines used for investigating flyrock distance.

Fig. 3. Pit bottom of a granite quarry and palm oil plantation surrounding the mine.

without gradient (Heidari et al., 2019). Therefore, it can overcome the disadvantages of the MLP model in finding the optimal structure and weights. To this end, the dataset was divided into two sections: 70% of the whole dataset was used for training the model and the remaining 30% was used for testing the performance of the developed model. In order to avoid model overfitting, the MinMax scaling method with the range of −1 to 1 was applied to normalizing the dataset. Subsequently, an initial MLP model was developed; then, the initial weights were encoded as a solution, and the HHO algorithm was applied to optimizing the weights of the developed MLP model. In other words, the HHO algorithm was utilized to train the MLP neural network to estimate flyrock distance in this study. During training the MLP model, different numbers of populations were considered, and the root mean squared error (RMSE) was used as the objective function to evaluate the optimization process of the HHO-MLP model. In this way, the HHO algorithm generated many solutions, and each solution was corresponding to a set of weights for the MLP model. Finally, the best set of weights was defined with the lowest RMSE, and it is the best model for predicting flyrock distance induced by mine blasting. The framework of the proposed HHO-MLP model to estimate flyrock is illustrated in Fig. 1.

The results of the HHO-MLP model then were compared with the other models, such as WOA-MLP, MLP (without optimization), SVM, RF and empirical models. The principle of HHO, WOA, MLP, SVM, and RF can be referred to the literature (Hearst et al., 1998; Breiman, 2001; Berk, 2008; Paliwal and Kumar, 2009; Mirjalili and Lewis, 2016; Gholami and Fakhari, 2017; Madhiarasan and Deepa, 2017; Mafarja and Mirjalili, 2017; Aljarah et al., 2018; Sun et al., 2018; Dewi and Chen, 2019; Gharehchopogh and Gholizadeh, 2019; Heidari et al., 2019, 2020; Moayedi et al., 2019; Yıldız and Yıldız, 2019; Joshi, 2020; Kamboj et al., 2020; Mirjalili et al., 2020; Tikhamarine et al., 2020).

3. Study site

This study was undertaken in three surface quarries located in Johor State (Malaysia). Their locations are shown in Fig. 2. The monthly production of these mines is 20,000 to 40,000 tons. Drilling and blasting method is adopted for the production of aggregates. There are residential areas and public roads within a distance of 400 m to 1 km from these quarries. Also, several palm oil plantations surround these mines, where plantation workers work during the daytime (Fig. 3). Therefore, flyrock induced by blasting operations in these mines is a major concern of engineers, mine operators, and surrounding communities. Since the selected quarries are located in a tropical area, weathering altered the rock mass significantly (Komoo, 1998; Tuğrul and Zarif, 1999), especially the physico-mechanical characteristics of rock mass (Tuğrul, 2004; Borrelli et al., 2014). Rock mass shall be categorized into different classes depending on the degree of weathering, i.e. fresh, slightly weathered, moderately weathered, highly weathered and completely weathered (Irfan and Dearman, 1978; Irfan and Powell, 1985; Tuğrul and Gürpinar, 1997; ISRM, 2007).

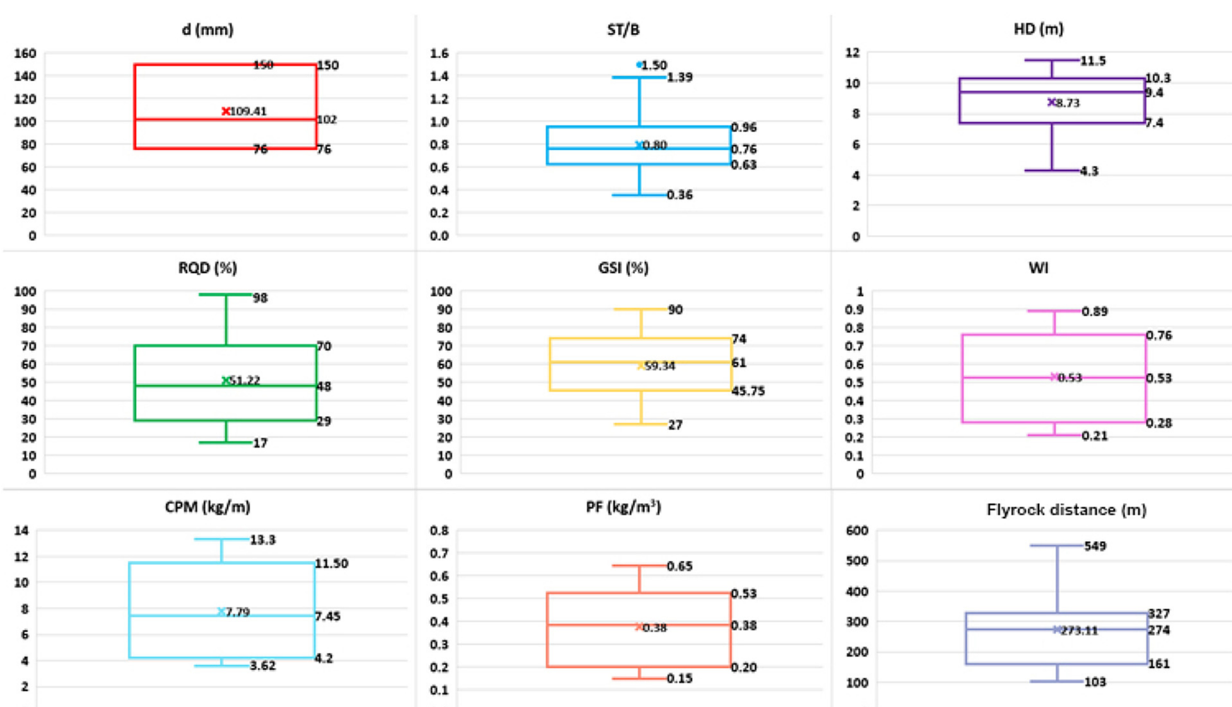

Fig. 4. Boxplots of input and output parameters.

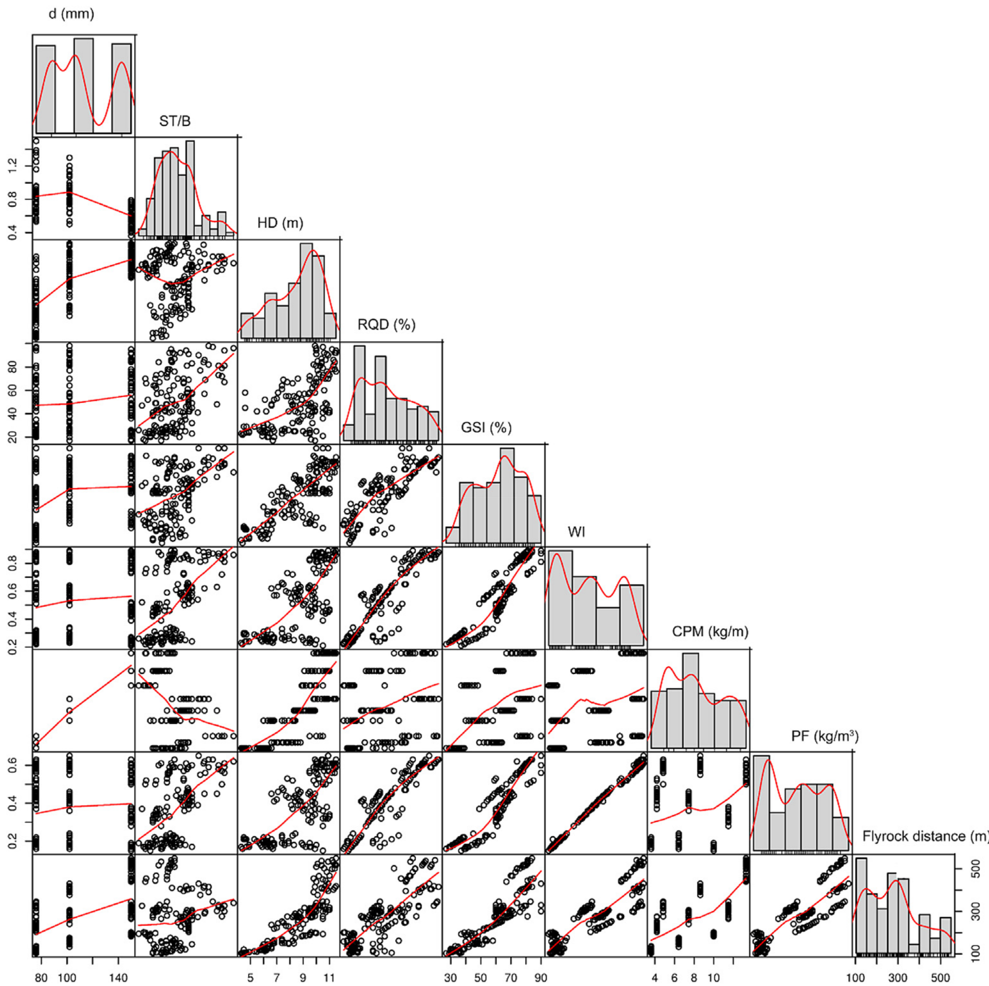

Fig. 5. Illustration of the dataset used, their density distributions, and the correlations between the input and output variables.

4. Dataset

In this study, 152 blasting operations were observed and pertinent data were compiled into a database. The collected data include measured flyrock distance, *d*, *GSI*, *WI*, *RQD*, *HD*, *ST*/*B*, *CPM* and *PF*. The data were divided into two groups: (i) uncertainty parameters, i.e. rock mass properties, and (ii) controllable parameters depending on blast design. The detailed boxplots of the dataset are illustrated in Figs. 4 and 5.

To detect the fly directions and locations of flyrock, a high-speed camera was used. Then, the locations of flyrock and blast sites were located using a Global Positioning System (GPS) device to calculate the flyrock distance. In blasting, design parameters in different blast patterns were considered as the controllable parameters, including *PF*, *d*, *HD*, *ST*/*B* and *CPM*. Of those, *d*, *B* and *ST* were measured with tape, *CPM* was computed using the explosives charged in each hole and its length, and *PF* was calculated based on the total explosives charged and volume of rock piles after blasting. As different drilling diameters were used at each of three quarries, blast design parameters are not consistent. *WI* was introduced based on three types of rock mass properties, i.e. water absorption, porosity and point load index. Completely weathered granite has the maximum water absorption and porosity values. Fresh granite has the maximum point load strength. Weathered granite samples were collected from the blasting face. Each property was compared with the respective maximum value to obtain a ratio. *WI* was then calculated based on the average of these three ratios for each blast.

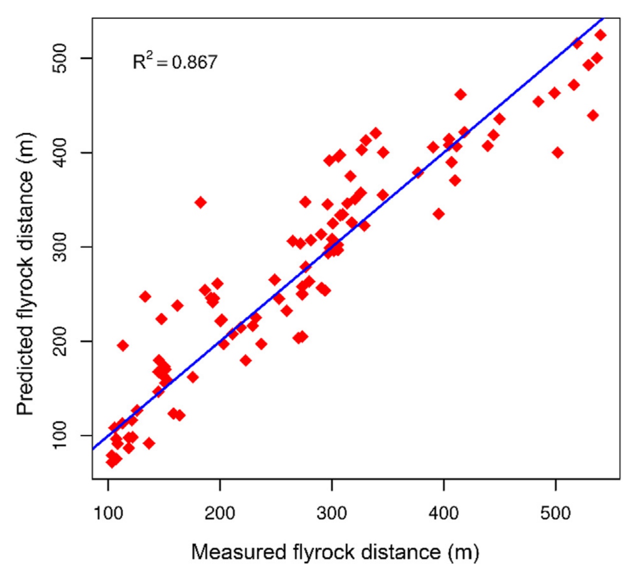

Fig. 6. The validity of the model through predicted versus actual flyrock values.

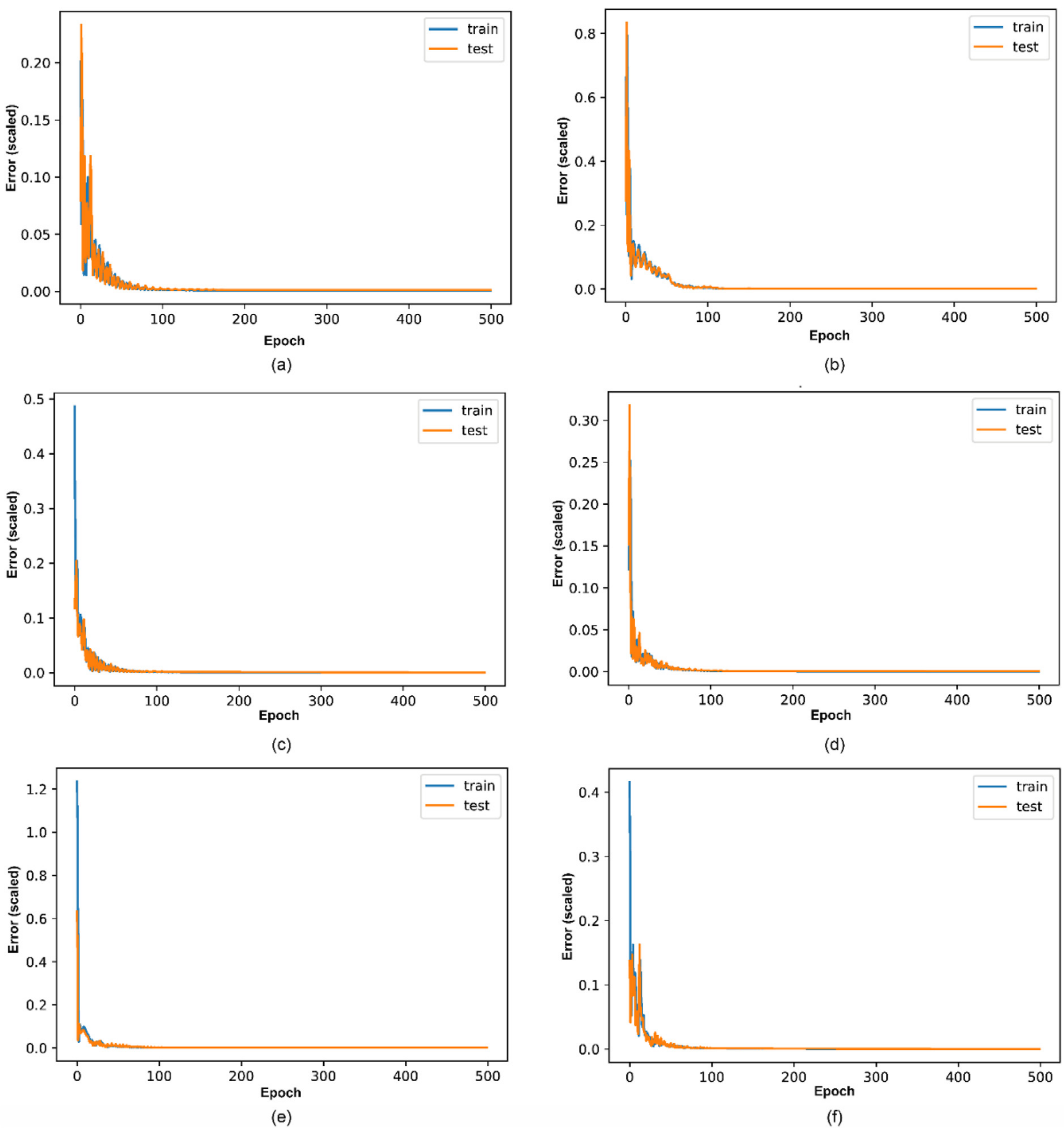

Fig. 7. Training/testing processes of the MLP models for predicting flyrock distance: (a) MLP 8-9-1, (b) MLP 8-12-1, (c) MLP 8-12-9-1, (d) MLP 8-15-12-1, (e) MLP 8-15-18-6-1, and (f) MLP 8-15-11-8-1.

In this study, *GSI* was determined after the blasting face was completely cleared by an excavator, and in situ granite can be observed before blasting. However, it must be noted that the average *GSI* value was used as an input parameter for predicting flyrock. *RQD* was determined by the scanline method (Babadagli, 2002) after the blasting face was cleared. The range of *RQD* is shown in Fig. 4 and its correlation is shown in Fig. 5. Accordingly, the correlation matrices between variables were presented through the relationship of paired variables and histograms. No variable has a normal distribution, and most of them have nonlinear relationships, except the correlation between *WI* and *PF*. Also, the correlations between *PF*, *GSI* and *RQD* are also positive, and they are good candidates for the predictive models. Other variables may have skewed and bimodal skewed distributions. Therefore, they may need to be normalized before being applied to the models.

5. Performance indices for the assessment of models

For evaluating the reliability and accuracy of the empirical and AI models, various indices were used to offer a comprehensive picture of the dataset used, as well as the errors of developed models. The assessment of models' performance was based on a variety of metrics, including a10-index, coefficient of determination (R^2), mean absolute percentage error (MAPE), variance accounted

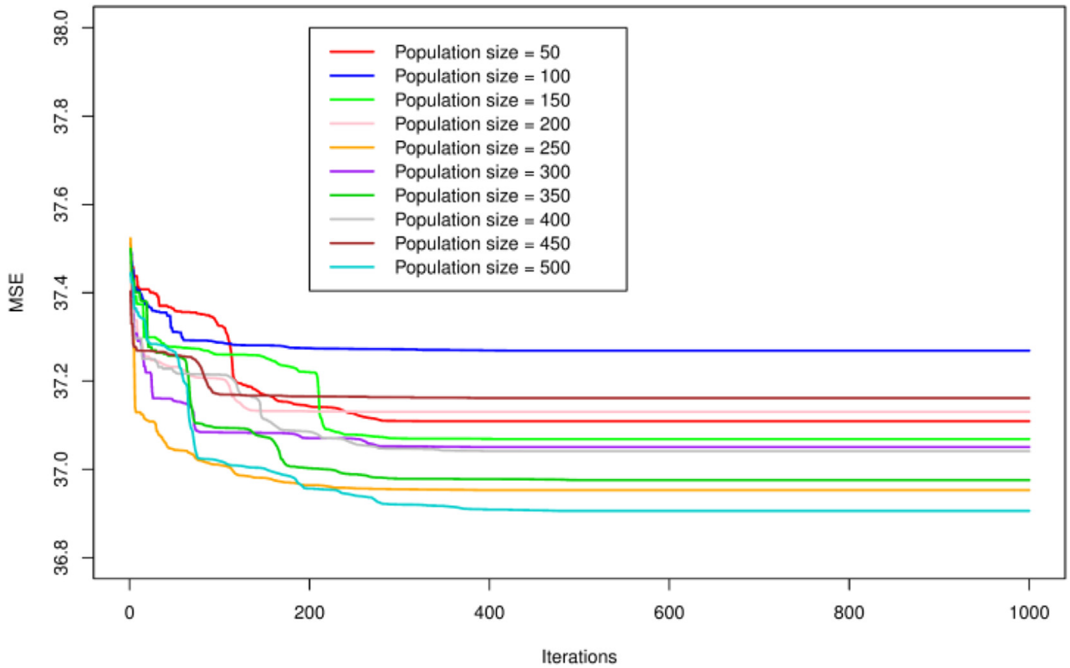

Fig. 8. Training process of the HHO-MLP model (optimization of the MLP model using the HHO algorithm).

for (VAF), RMSE, and root squared error (RSE). The equations for these indices are presented below:

$$R^2 = 1 - \frac{\sum_{i=1}^{N}(z - z')^2}{\sum_{i=1}^{N}(z - \bar{z})^2} \tag{1}$$

$$MAPE = \frac{\sum_{i=1}^{N}\left|\frac{z-z'}{z}\right|}{N} \times 100 \tag{2}$$

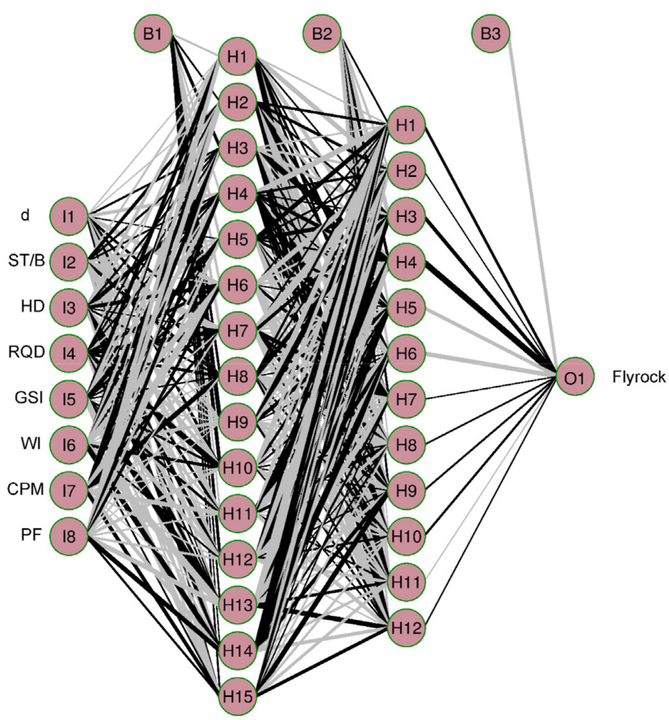

Fig. 9. The structure of the HHO-MLP model for predicting flyrock distance.

$$VAF = \left[1 - \frac{\mathrm{var}(z - z')}{\mathrm{var}(z)}\right] \times 100 \tag{3}$$

$$RMSE = \sqrt{\frac{1}{N}\sum_{i=1}^{N}(z - z')^2} \tag{4}$$

$$RSE = \frac{\sum_{i=1}^{N}(z' - z)^2}{\sum_{i=1}^{N}(\bar{z} - z)^2} \tag{5}$$

where z and z' are the measured and predicted values, respectively; $\bar{z}$ is the mean of the measured z values; and N is the number of total samples. In theory, the model is exceptional if R^2 is 1, VAF is 100%, and RMSE, MAPE and mean squared error (MSE) are 0. In addition, a10-index is one of the latest statistical index used by many researchers for evaluation of the AI/ML models (Duan et al., 2020; Zhou et al., 2021):

$$a10 - index = \frac{m^{10}}{M} \tag{6}$$

where M represents the amount of dataset samples, m^{10} denotes the rate of experimental/predicted value that lies between the range of 0.9–1.1.

Furthermore, to assess the effect of geological parameters of rock mass and controllable parameters of blasting, the Taylor diagram and sensitivity analysis method were applied. These indices are well known and commonly used and the formulae for calculating these indices are available in various literature.

6. Developing the models for predicting flyrock distance

Six computational models were developed to estimate flyrock distance, including the empirical, MLP, HHO-MLP, WOA-MLP, SVM, and RF models. To develop these models, the dataset with 152 blasting events was randomly separated into two sections: (i) 70%

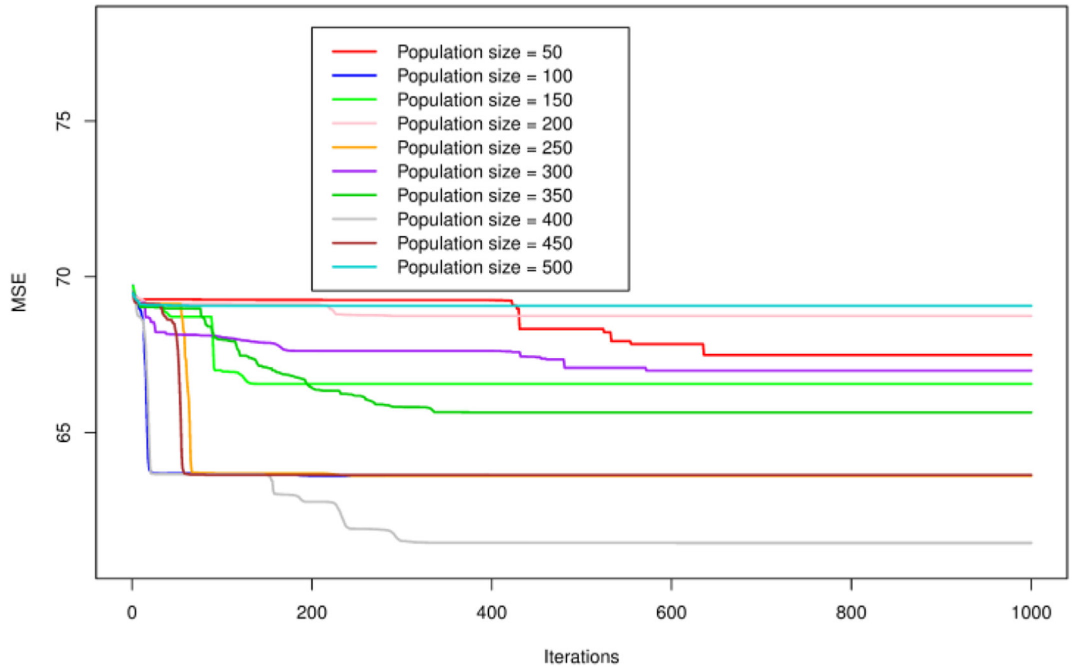

Fig. 10. Training process of the WOA-MLP model (optimization of the MLP model using WOA).

for training, and (ii) 30% for testing. All the models were developed using similar training and testing dataset.

6.1. Empirical model

In order to develop the empirical model based on blast design and geological parameters, there are many models available over the years. Their accuracy depends on the input parameters, as well as the

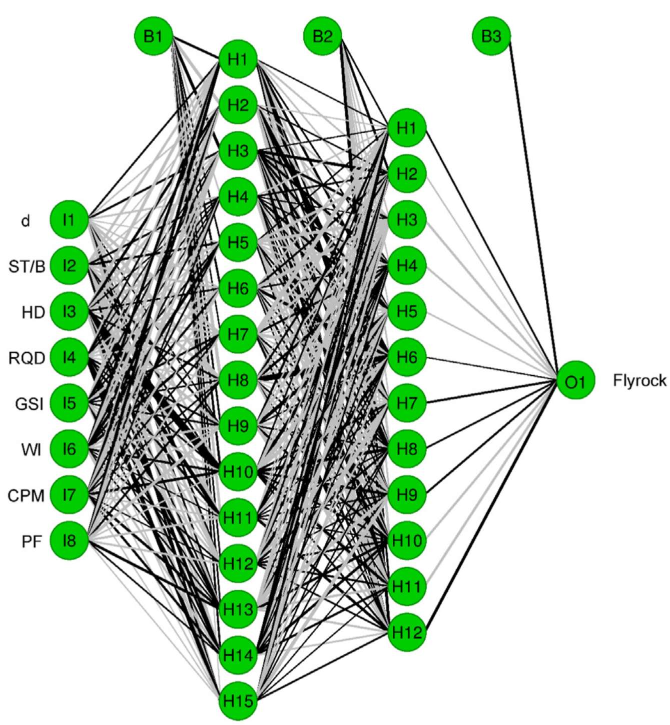

Fig. 11. The structure of the WOA-MLP model for estimating flyrock distance.

dataset of field observations used in the analysis (Lundborg et al., 1975; Bagchi and Gupta, 1990; Olofsson, 1990; Moore and Richards, 2004; Little, 2007; Ghasemi et al., 2012; Trivedi et al., 2014; Armaghani et al., 2016b). As introduced in the instruction section, Lundborg et al. (1975) and Bagchi and Gupta (1990) claimed that the borehole diameter (d) has a significant effect on flyrock distance. Olofsson (1990) and Trivedi et al. (2014) indicated that ST/B and RQD have a great effect on the distance of flyrock as well. Therefore, we proposed an empirical formula for estimating flyrock distance using d, ST/B and RQD. The multivariate linear regression method was used to identify the relationship of these parameters. Finally, an empirical equation for estimating flyrock distance was found, as presented in Eq. (7). Fig. 6 shows the validity of the model through predicted versus actual graph with 1:1 line and R^2.

$$\text{Flyrock distance} = 2.421\ d + 95.479\ ST/B + 3.503\ RQD - 243.139 \tag{7}$$

6.2. MLP models

For the development of the MLP model, the structure of MLP, including the number of hidden layers and neurons, is the major concern. Numerous previous researchers proposed the formulae to calculate the number of hidden layers and neurons (Yi and Ge, 2005; Trenn, 2008; Sheela and Deepa, 2013); however, their performance varies significantly in different cases (Alsmadi et al., 2009; Kuo et al., 2009). Many other scholars recommended that the "trial-and-error" technique as the best approach to determine the structure of the MLP model (Chauhan et al., 2012; Thota and Changalasetty, 2013; Assi et al., 2018; Itano et al., 2018). Hence, a "trial-and-error" method for selection of the hidden layers and neurons of MLP model was implemented to determine the best MLP model in predicting flyrock distance. Six MLP models with one to three hidden layers and different numbers of neurons were investigated. Note that the backpropagation algorithm was used to train MLP models, and the MSE was utilized as the objective

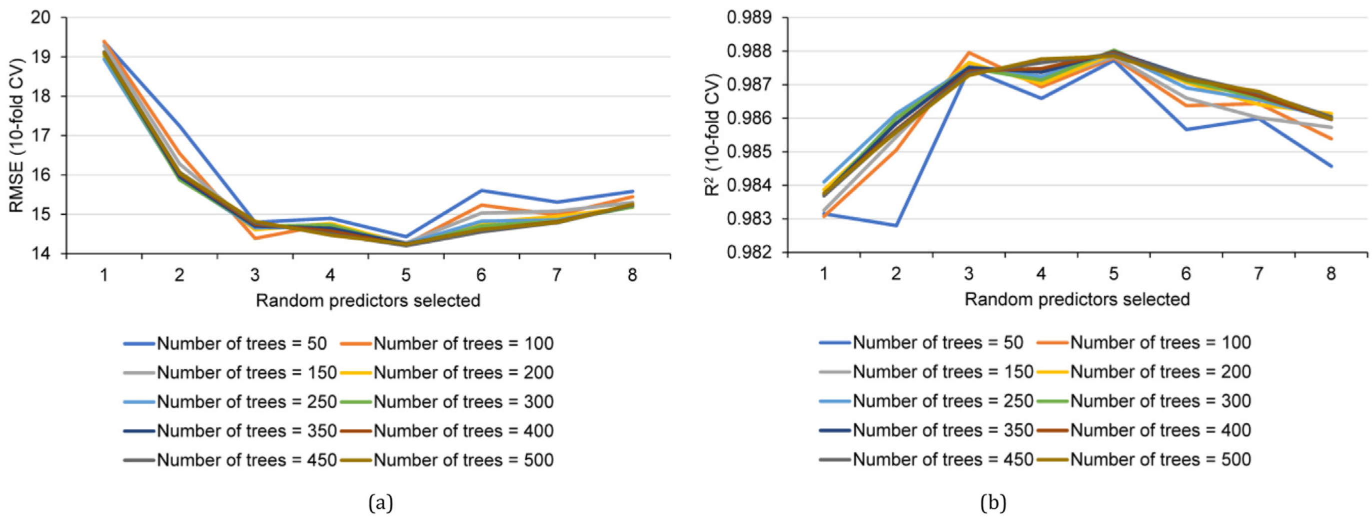

Fig. 12. Performance of RF models with different hyper-parameters: (a) Evaluation of RF models using RMSE, and (b) Evaluation of RF models based on R^2.

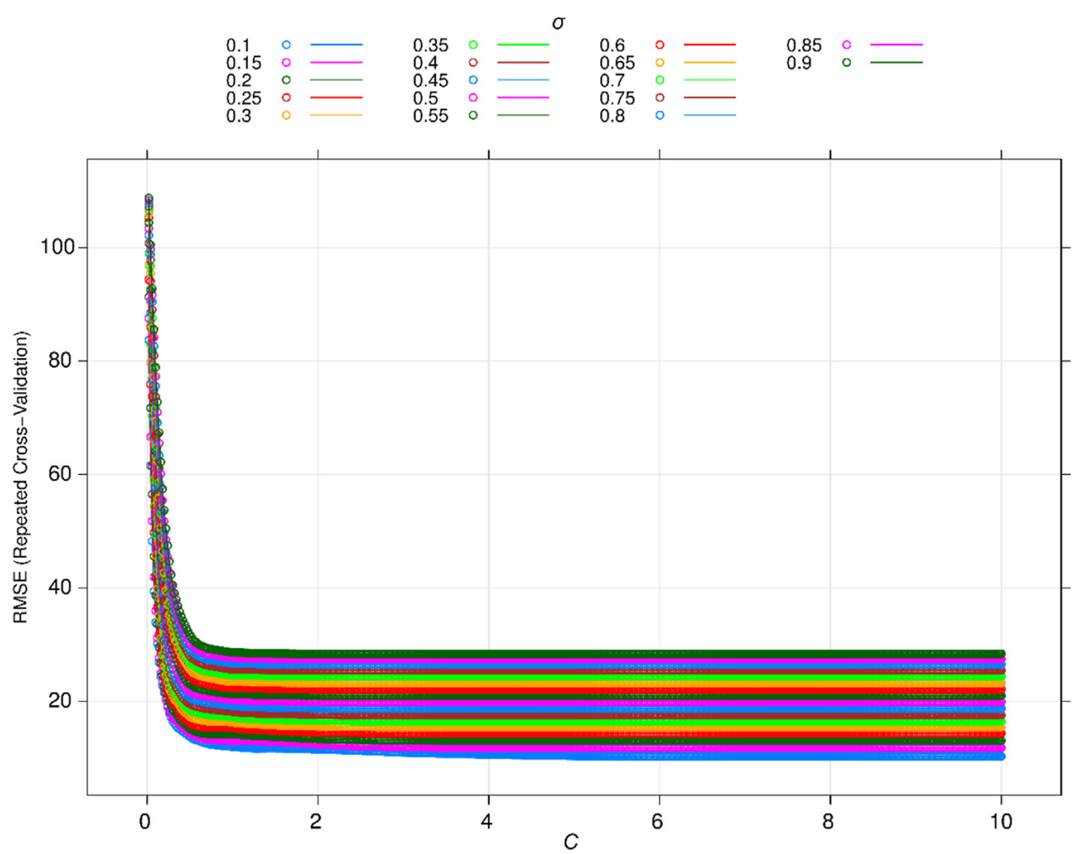

Fig. 13. Performance of the SVM model with different hyper-parameters.

function during the training process. The training process of MLP model is illustrated in Fig. 7. Finally, the MLP 8-15-12-1 (8 neurons in the input layer, 15 neurons in the first hidden layer, 12 neurons in the second hidden layer, and 1 neuron in the output layer) was found as the best MLP model. It can explain the relationship between the geological parameters of rock mass, controllable parameters of blasting, and flyrock distance well.

6.3. HHO-MLP model

For the HHO-MLP modeling, the framework proposed in Fig. 1 was applied based on the same training dataset. In the first phase, an MLP model was developed as the main element for the optimization of the HHO algorithm. Since the MLP 8-15-12-1 was tested as the best MLP model, it was selected as the initial MLP

Fig. 14. The comparison of predicted versus measured flyrock distances.

Table 2
Comparison of the performance of predictive models on the training and testing datasets.

Model	Training dataset						Testing dataset					
	a10-index	R^2	RMSE	MAPE	VAF	RSE	a10-index	R^2	RMSE	MAPE	VAF	RSE
WOA-MLP	0.972	0.996	7.840	0.026	99.612	0.0002	0.978	0.995	9.21	0.028	99.469	0.0028
HHO-MLP	**0.991**	**0.998**	**6.075**	**0.019**	**99.767**	**0.0007**	**0.978**	**0.996**	**7.205**	**0.026**	**99.636**	**0.0051**
MLP	0.953	0.996	8.055	0.029	99.591	0.0026	0.935	0.994	9.664	0.032	99.379	0.0098
SVM	0.937	0.994	10.339	0.034	99.328	0.0028	0.935	0.996	8.096	0.029	99.55	0.03
RF	0.933	0.988	14.202	0.047	98.824	0.0051	0.935	0.929	12.802	0.038	98.811	0.017
Empirical	0.575	0.867	46.624	0.13	88.539	0.032	0.413	0.855	47.438	0.172	85.108	0.128

Note: The best predictive model for flyrock distance is shown in bold.

model for the development of the HHO-MLP model. During the second phase, the HHO algorithm implements the optimization of the selected MLP model including weights and biases.

To carry out the second phase, the parameters of the HHO algorithm were defined first. As required in the pseudo-code of the HHO algorithm (Heidari et al., 2019), the maximum number of iterations (T) and population size (N) are prerequisite parameters for the HHO algorithm. To assess the HHO algorithm's performance in optimizing the selected MLP model (i.e. the HHO-MLP model), different N values were selected as 50, 100, 150, 200, 250, 300, 350, 400, 450 and 500 with $T = 1000$. MSE was also utilized as the stopping condition in the optimization process of the HHO-MLP model. Finally, the ideal HHO-MLP model was reached at the iteration of 461, as shown in Fig. 8. The optimal structure, as well as optimal weights of the selected MLP model, are presented in Fig. 9.

6.4. WOA-MLP model

The function of WOA is the same as the HHO algorithm. It means that the WOA implements an optimization task for the selected MLP model. It must be noted that the required parameters of WOA are the same as the HHO algorithm. Therefore, they were selected as those used for the HHO algorithm. The training performance of the WOA-MLP model is shown in Fig. 10, and its structure is illustrated in Fig. 11. It is worth noting that whereas Fig. 9 shows the structure of the HHO-MLP model, Fig. 11 shows the structure of the WOA-MLP model. The main difference between these two figures is the weights of the models, and they are shown through the black and grey lines, as well as the thickness of the lines.

6.5. RF model

To develop the RF model, the number of trees and random predictors chosen are the parameters applied to controlling the accuracy of the RF model. Of those, the accuracy of the RF model is highly dependent on the number of trees since RF is a decision tree-based algorithm. Hence, a trial-and-error method was implemented with the number of trees of 50, 100, 150, 200, 250, 300, 350, 400, 450 and 500. Also, since the predictor used is 8 (8 input variables), the random predictors were also selected in the range of 1–8. Note that 10-fold cross-validation (CV) and Box-Cox transformation techniques were used as well to prevent overfitting of the RF model. RMSE and R^2 were utilized to evaluate the performance of RF models with different parameters, as demonstrated in Fig. 12. Finally, the ideal RF model was defined with the number of trees of 450, and the random predictors was selected at 5.

6.6. SVM model

Similar to other models, the performance of the SVM model was also controlled by hyper-parameters. As mentioned above, kernel functions shall be used to map the dataset to improve the performance of support vectors. For this problem, the radius basis function (RBF) was commonly recommended for SVM models in engineering problems (Bui et al., 2019a, b, c; Guo et al., 2019a, b; Nguyen, 2019; Nguyen et al., 2019d, 2020; Lv et al., 2020). Therefore, σ and cost (C) were utilized to control the accuracy of the SVM model in estimating flyrock distance. The best parameters of the SVM model were selected using the grid search technique, as

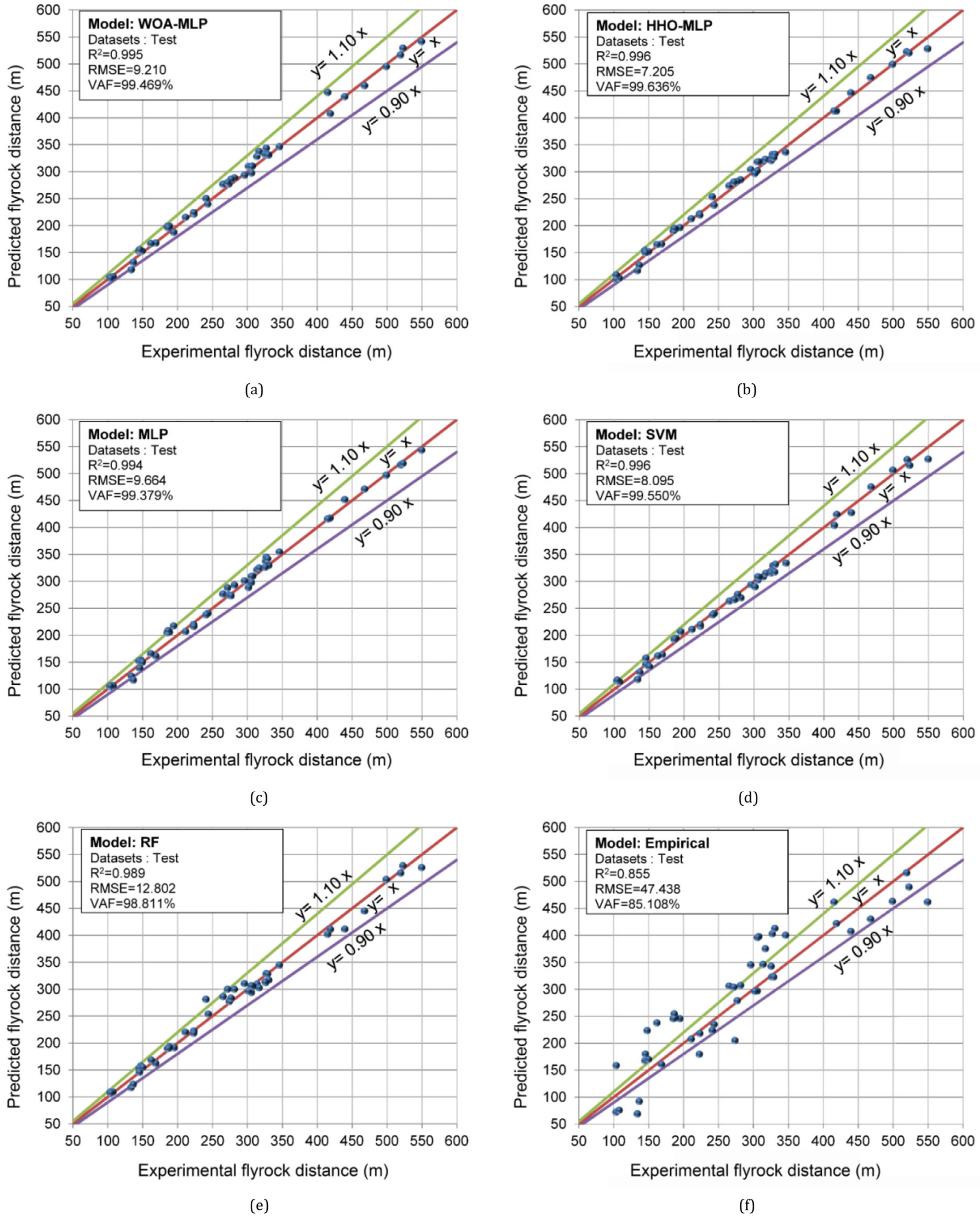

Fig. 15. Predicted versus measured flyrock distances by different predictive models: (a) HHO-MLP model, (b) WOA-MLP model, (c) MLP model, (d) SVM model, (e) RF model, and (f) Empirical model.

illustrated in Fig. 13. It must be noted that 10-fold CV and Box-Cox transformation techniques were used as well to prevent overfitting of the SVM model. Herein, 10-fold CV was repeated 3 times to evaluate the model's performance. Eventually, the ideal SVM model was defined with $C = 5.96$ and $\sigma = 0.1$.

7. Results

In modeling flyrock distance, the predictive ability of the developed models should be assessed properly. In this study, all predictive models were developed using the same training dataset.

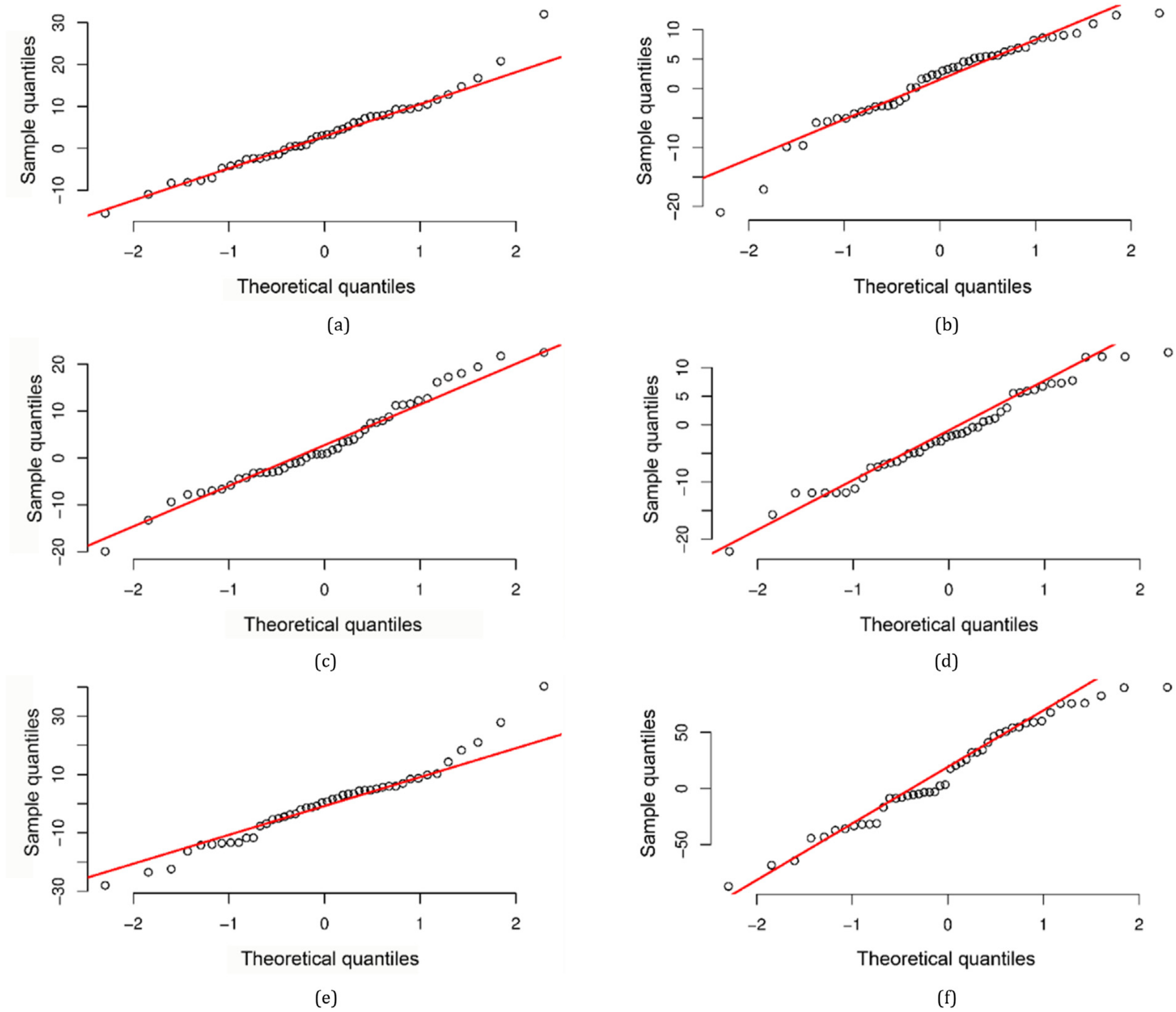

Fig. 16. Normal Q-Q plots of each model for evaluating the fitness of the models: (a) HHO-MLP model, (b) WOA-MLP model, (c) MLP model, (d) SVM model, (e) RF model, and (f) Empirical model.

Subsequently, the testing dataset was utilized to evaluate the predictive ability of developed models. The output of the predictive models using the testing dataset is shown in Fig. 14, and their performance is outlined in Table 2.

8. Discussion

The findings of this study indicated that the AI models outperformed the empirical model in predicting flyrock at three granite mines in Malaysia. It must be noted that all the AI models worked effectively on both training and testing datasets. Particularly, the overfitting problem did not occur with these models. Of the five AI models, the HHO-MLP model provided the best performance with R^2 of 0.996, RMSE of 7.205, VAF of 99.636, and MAPE of 0.026 on the testing dataset. However, the remaining AI models provided lower performance with R^2 of 0.929–0.996, RMSE of 8.096–12.802, VAF of 98.811–99.55, and MAPE of 0.028–0.038, on the testing dataset. It is worth mentioning that the performance of the WOA- MLP model is also better than those of the single MLP model (without optimization). However, it is lower compared to the SVM model. This finding indicated that the HHO algorithm is better than the WOA algorithm in the optimization of the MLP model. By examining all proposed AI models, RF provided the worst performance. Fig. 15 shows the further assessment of developed models on the testing dataset.

The relationship between measured and predicted values by the developed models with the 90% confidence level is depicted in Fig. 15. The AI models provided high convergences, especially the proposed HHO-MLP model with all the data points within the 90% confidence level. Meanwhile, most of the data points of the empirical models are outside of the 90% confidence level. These results demonstrated the dominant performance of the AI models in predicting flyrock distance, especially the proposed HHO-MLP model. This finding indicated that the AI models, especially the proposed HHO-MLP model, can better explain the relationship between the geological parameters of rock mass, controllable parameters of blasting, and flyrock distance than other models.

Normal quantiles-quantiles (*Q-Q*) plots were used to demonstrate the fitness of developed models based on the dataset used. The results show whether the outcome of the predictions have normal distribution or not. From the data science and machine learning perspectives, the normal distribution is considered an important statistical feature since it fits many natural phenomena. Thus, the deviations of data (in this study, flyrock distance) from a normal distribution shall be utilized to estimate the accuracy of machine learning algorithms (Lu et al., 2019; Nagano et al., 2019;

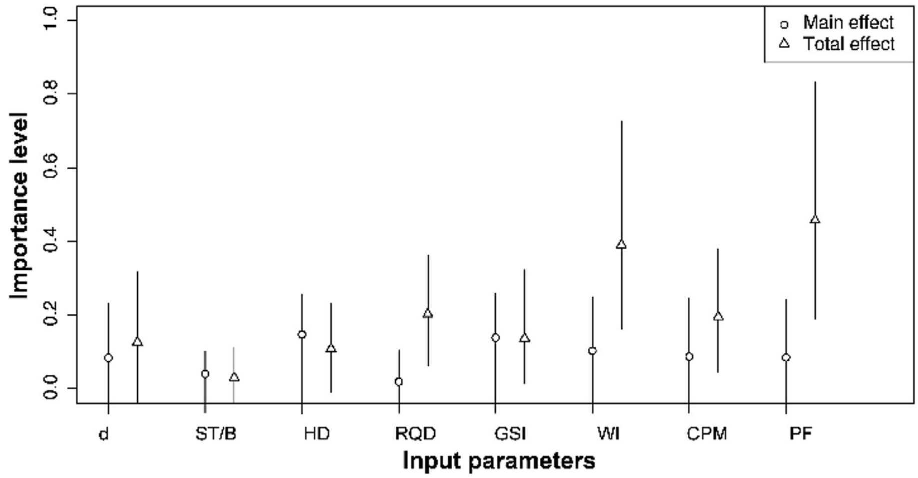

Fig. 17. Evaluation of the influence of various input variables on flyrock distance.

Salas-Rueda 2019). Fig. 16 presents the normal distribution of the residuals of the developed models based on the testing dataset using *Q-Q* plots. From Fig. 16, it is found that most of the developed models have a potential normal distribution based on the residuals of the testing dataset. However, taking a closer look at Fig. 16, it shows that the HHO-MLP and WOA-MLP models exhibit better normal distribution compared to other models. In other words, the HHO-MLP and WOA-MLP models offer better fits than the other models. Of those, the normal distribution of the HHO-MLP is slightly better than the WOA-MLP model.

Although the accuracy and reliability of the proposed HHO-MLP were demonstrated as the most superior, the impact of input parameters on flyrock should be checked to ensure that correct trends in input and output data would be established. Furthermore, the sensitivity analysis determines the impact of each input variable on the accuracy of the predictive model. The sensitivity analysis was carried out for the HHO-MLP model based on the Sobol method (Nossent et al., 2011; Rosolem et al., 2012; Wan et al., 2015), as shown in Fig. 17. The sensitivity analysis results showed that the uncertainty parameters have significant effects on flyrock distance, especially *WI*, *GSI* and *RQD*. In other words, not only blasting parameters but also rock mass properties have significant effects on flyrock distance induced by mine blasting. The primary parameters should be considered to have a comprehensive assessment of the influential parameters on flyrock distance in blasting operations, especially in the tropically weathered granite and other types of rocks.

9. Conclusions

Flyrock is a hazardous phenomenon induced by blasting events in open-pit mines. An empirical and five AI models were developed for the prediction of flyrock. This study proposed a robust combination of the HHO algorithm and MLP model (i.e. HHO-MLP) in predicting flyrock to increase the accuracy of the MLP model. The performance of the suggested HHO-MLP model was compared with various soft computing models, such as WOA-MLP, MLP (without optimization), SVM, RF and empirical models. It showed that the performance of the proposed HHO-MLP model is the best with the highest accuracy.

Based on the obtained results of the developed models, although the empirical models are simpler and easier to apply in practice, their accuracies are poorer than those of the soft computing models, especially the proposed HHO-MLP model. From the modeling perspective, hybrid models are often more complex than standalone models; however, once the hybrid model (i.e. HHO-MLP) was well-developed, its application is the same as the other models, and it is useful in practical engineering.

All eight input parameters affected flyrock distance, while their importance levels are different. It is worth noting that the rock mass properties also have significant effects on flyrock distance induced by mine blasting, especially *WI*, *GSI* and *RQD*. The models proposed are based on data from several specific sites (in Malaysia); therefore, the obtained results may not be suitable for other geological settings, i.e. in limestone or other quarries. Future research with the consideration of the blastability index, *WI*, and other controllable parameters of blast design can improve the accuracy and reliability of the prediction models.

Declaration of competing interest

The authors declare that they have no known competing financial interests or personal relationships that could have appeared to influence the work reported in this paper.

Acknowledgments

This study was supported by the Center for Mining, Electro-Mechanical Research of Hanoi University of Mining and Geology (HUMG), Hanoi, Vietnam. The authors are also thankful to Prof. Dr. Edy Tonnizam, Director of Geotropik, Universiti Teknologi Malaysia for providing useful technical information/data and encouragement for conducting this research.

References

Aljarah, I., Faris, H., Mirjalili, S., 2018. Optimizing connection weights in neural networks using the whale optimization algorithm. Soft Comput 22 (1), 1–15.

Alsmadi, M.K., Omar, K.B., Noah, S.A., Almarashdah, I., 2009. Performance comparison of multi-layer perceptron (Back Propagation, Delta Rule and Perceptron) algorithms in neural networks. 2009 IEEE International Advance Computing Conference. IEEE, pp. 296–299.

Armaghani, D.J., Hajihassani, M., Mohamad, E.T., Marto, A., Noorani, S., 2014. Blasting-induced flyrock and ground vibration prediction through an expert artificial neural network based on particle swarm optimization. Arab. J. Geosci. 7 (12), 5383–5396.

Armaghani, D.J., Mahdiyar, A., Hasanipanah, M., Faradonbeh, R.S., Khandelwal, M., Amnieh, H.B., 2016a. Risk assessment and prediction of flyrock distance by combined multiple regression analysis and Monte Carlo simulation of quarry blasting. Rock Mech. Rock Eng. 49 (9), 3631–3641.

Armaghani, D.J., Mohamad, E.T., Hajihassani, M., Abad, S.A.N.K., Marto, A., Moghaddam, M., 2016b. Evaluation and prediction of flyrock resulting from

blasting operations using empirical and computational methods. Eng. Comput. 32 (1), 109–121.
Asl, P.F., Monjezi, M., Hamidi, J.K., Armaghani, D.J., 2018. Optimization of flyrock and rock fragmentation in the Tajareh limestone mine using metaheuristics method of firefly algorithm. Eng. Comput. 34 (2), 241–251.
Assi, K.J., Nahiduzzaman, K.M., Ratrout, N.T., Aldosary, A.S., 2018. Mode choice behavior of high school goers: evaluating logistic regression and MLP neural networks. Case Stud. Transp. Policy. 6 (2), 225–230.
Babadagli, T., 2002. Scanline method to determine the fractal nature of 2-d fracture networks. Math. Geol. 34 (6), 647–670.
Bagchi, A., Gupta, R., 1990. Surface blasting and its impact on environment. In: Workshop on Environmental Management of Mining Operations, Varanasi 1990, pp. 262–279.
Bahrami, A., Monjezi, M., Goshtasbi, K., Ghazvinian, A., 2011. Prediction of rock fragmentation due to blasting using artificial neural network. Eng. Comput. 27 (2), 177–181.
Berk, R.A., 2008. Random forests. In: Statistical Learning from a Regression Perspective. Springer, pp. 1–63.
Bhandari, S., 1997. Engineering Rock Blasting Operations. A.A. Balkema, Rotterdam, Netherlands.
Bhowmik, S., Raina, A.K., Chakraborty, A.K., Ramulu, M., Sahu, P.B., Haldar, A., Choudhury, P., 2004. Flyrock prediction and control in opencast mines: a critical appraisal. Min. Eng. J. 6 (5), 10–20.
Borrelli, L., Perri, F., Critelli, S., Gullà, G., 2014. Characterization of granitoid and gneissic weathering profiles of the Mucone River basin (Calabria, southern Italy). Catena 113, 325–340.
Bui, H.B., Nguyen, H., Choi, Y., Bui, X.N., Nguyen-Thoi, T., Zandi, Y., 2019a. A novel artificial intelligence technique to estimate the gross calorific value of coal based on meta-heuristic and support vector regression algorithms. Appl. Sci. 9 (22), 4868.
Bui, X.N., Lee, C.W., Nguyen, H., Bui, H.B., Long, N.Q., Le, Q.T., Nguyen, V.D., Nguyen, N.B., Moayedi, H., 2019b. Estimating PM10 concentration from drilling operations in open-pit mines using an assembly of SVR and PSO. Appl. Sci. 9 (14), 2806.
Bui, X.N., Nguyen, H., Le, H.A., Bui, H.B., Do, N.H., 2019c. Prediction of blast-induced air over-pressure in open-pit mine: assessment of different artificial intelligence techniques. Nat. Resour. Res. 29 (2), 571–591.
Breiman, L., 2001. Random forests. Mach. Learn. 45 (1), 5–32.
Chauhan, S., Goel, V., Dhingra, S., 2012. Pattern recognition system using MLP neural networks. Pattern Recogn. 4 (9), 43–46.
Chen, Z., Li, H., Goh, A.T.C., Wu, C., Zhang, W., 2020. Soil liquefaction assessment using soft computing approaches based on capacity energy concept. Geosci. 10 (9), 330.
De Silva, D., Sierla, S., Alahakoon, D., Osipov, E., Yu, X., Vyatkin, V., 2020. Toward intelligent industrial informatics: a review of current developments and future directions of artificial intelligence in industrial applications. IEEE Ind. Electron. Mag. 14 (2), 57–72.
Dewi, C., Chen, R.C., 2019. Random forest and support vector machine on features selection for regression analysis. Int. J. Innov. Comput. Inf. Control 15 (6), 2027–2037.
Duan, J., Asteris, P.G., Nguyen, H., Bui, X.N., Moayedi, H., 2020. A novel artificial intelligence technique to predict compressive strength of recycled aggregate concrete using ICA-XGBoost model. Eng. Comput. 37, 3329–3346.
Faradonbeh, R.S., Armaghani, D.J., Monjezi, M., Mohamad, E.T., 2016. Genetic programming and gene expression programming for flyrock assessment due to mine blasting. Int. J. Rock Mech. Min. Sci. 88, 254–264.
Finn, O., Ulf, N., Mats, O., Ingvar, B., Lars, G., Henrik, G., 2004. Where does the explosive energy in rock blasting rounds go? Sci. Technol. Energetic Mater. 65, 54–63.
Gharehchopogh, F.S., Gholizadeh, H., 2019. A comprehensive survey: whale Optimization Algorithm and its applications. Swarm Evol. Comput. 48, 1–24.
Ghasemi, E., Sari, M., Ataei, M., 2012. Development of an empirical model for predicting the effects of controllable blasting parameters on flyrock distance in surface mines. Int. J. Rock Mech. Min. Sci. 52, 163–170.
Gholami, R., Fakhari, N., 2017. Support vector machine: principles, parameters, and applications. In: Handbook of Neural Computation. Elsevier, pp. 515–535.
Guo, H.Q., Nguyen, H., Bui, X.N., Armaghani, D.J., 2019a. A new technique to predict fly-rock in bench blasting based on an ensemble of support vector regression and GLMNET. Eng. Comput. 37 (1), 421–435.
Guo, H.Q., Nguyen, H., Vu, D.A., Bui, X.N., 2019b. Forecasting mining capital cost for open-pit mining projects based on artificial neural network approach. Res. Pol. 101474. https://doi.org/10.1016/j.resourpol.2019.101474.
Han, H., Armaghani, D.J., Tarinejad, R., Zhou, J., Tahir, M.M., 2020. Random forest and bayesian network techniques for probabilistic prediction of flyrock induced by blasting in quarry sites. Nat. Resour. Res. 29 (2), 655–667.
Hasanipanah, M., Armaghani, D.J., Amnieh, H.B., Majid, M.Z.A., Tahir, M.M., 2017. Application of PSO to develop a powerful equation for prediction of flyrock due to blasting. Neural Comput. Appl. 28 (1), 1043–1050.
Hasanipanah, M., Armaghani, D.J., Amnieh, H.B., Koopialipoor, M., Arab, H., 2018. A risk-based technique to analyze flyrock results through rock engineering system. Geotech. Geol. Eng. 36 (4), 2247–2260.
Hasanipanah, M., Amnieh, H.B., 2020. A fuzzy rule-based approach to address uncertainty in risk assessment and prediction of blast-induced flyrock in a quarry. Nat. Resour. Res. 29 (2), 669–689.
Hearst, M.A., Dumais, S.T., Osuna, E., Platt, J., Scholkopf, B., 1998. Support vector machines. IEEE Intell. Syst. Their Appl. 13 (4), 18–28.
Heidari, A.A., Mirjalili, S., Faris, H., Aljarah, I., Mafarja, M., Chen, H.L., 2019. Harris hawks optimization: algorithm and applications. Future Generat. Comput. Syst. 97, 849–872.
Heidari, A.A., Faris, H., Mirjalili, S., Aljarah, I., Mafarja, M., 2020. Ant lion optimizer: theory, literature review, and application in multi-layer perceptron neural networks. In: Nature-inspired Optimizers. Springer, pp. 23–46.
Hudaverdi, T., Akyildiz, O., 2019. A new classification approach for prediction of flyrock throw in surface mines. Bull. Eng. Geol. Environ. 78 (1), 177–187.
Irfan, T.Y., Powell, G.E., 1985. Engineering geological investigations for pile foundations on a deeply weathered granitic rock in Hong Kong. Bull. Int. Assoc. Eng. Geol. -Bulletin de l'Association Internationale de Géologie de l'Ingénieur. 32 (1), 67–80.
Irfan, T.Y., Dearman, W.R., 1978. Engineering classification and index properties of a weathered granite. Bull. Int. Assoc. Eng. Geol. -Bulletin de l'Association Internationale de Géologie de l'Ingénieur. 17 (1), 79–90.
ISRM (International Society for Rock Mechanics), 2007. The complete ISRM suggested methods for rock characterization, testing and monitoring: 1974–2006. In: Ulusay, R., Hudson, J.A. (Eds.), Suggested Methods Prepared by the Commission on Testing Methods. International Society for Rock Mechanics, Compilation Arranged by the ISRM Turkish National Group. Kozan Ofset, Ankara, Turkey.
Itano, F., de Abreu de Sousa, M.A., Del-Moral-Hernandez, E., 2018. Extending MLP ANN hyper-parameters optimization by using genetic algorithm. 2018 International Joint Conference on Neural Networks (IJCNN). IEEE, pp. 1–8.
Joshi, A.V., 2020. Support vector machines. In: Machine Learning and Artificial Intelligence. Springer, pp. 65–71.
Kamboj, V.K., Nandi, A., Bhadoria, A., Sehgal, S., 2020. An intensify Harris Hawks optimizer for numerical and engineering optimization problems. Appl. Soft Comput. 89, 106018.
Khandelwal, M., 2011. Blast-induced ground vibration prediction using support vector machine. Eng. Comput. 27 (3), 193–200.
Khandelwal, M., Singh, T.N., 2005. Prediction of blast induced air overpressure in opencast mine. Noise Vib. Worldw. 36 (2), 7–16.
Komoo, I., 1998. Deep weathering: major cause of slope failure in wet tropical terrain. In: Engineering Geology: A Global View from the Pacific Rim. A.A. Balkema, Rotterdam, Netherlands, pp. 1773–1778.
Kuo, Y.L., Jaksa, M.B., Lyamin, A.V., Kaggwa, W.S., 2009. ANN-based model for predicting the bearing capacity of strip footing on multi-layered cohesive soil. Comput. Geotech. 36 (3), 503–516.
Li, B.H., Hou, B.C., Yu, W.T., Lu, X.B., Yang, C.W., 2017. Applications of artificial intelligence in intelligent manufacturing: a review. Front. Inf. Technol. Electron. Eng. 18 (1), 86–96.
Little, T.N., 2007. Flyrock risk. In: Proceedings EXPLO 2007. Wollongong, New South Wales, Australia, pp. 35–43.
Liu, R.N., Yang, B.Y., Zio, E., Chen, X.F., 2018. Artificial intelligence for fault diagnosis of rotating machinery: a review. Mech. Syst. Signal Process. 108, 33–47.
Lu, H.J., Zou, N., Jacobs, R., Afflerbach, B., Lu, X.G., Morgan, D., 2019a. Error assessment and optimal cross-validation approaches in machine learning applied to impurity diffusion. Comput. Mater. Sci. 169, 109075. https://doi.org/10.1016/j.commatsci.2019.06.010.
Lu, X., Hasanipanah, M., Brindhadevi, K., Amnieh, H.B., Khalafi, S., 2019b. ORELM: a novel machine learning approach for prediction of flyrock in mine blasting. Nat. Resour. Res. 29 (2), 641–654.
Lundborg, N., Persson, A., Ladegaard-Pedersen, A., Holmberg, R., 1975. Keeping the lid on flyrock in open-pit blasting. Eng. Min. J. 176, 95–100.
Lv, Y.L., Le, Q.T., Bui, H.B., Bui, X.N., Nguyen, H., Nguyen-Thoi, T., Dou, J., Song, X., 2020. A comparative study of different machine learning algorithms in predicting the content of ilmenite in titanium placer. Appl. Sci. 10 (2), 635.
Mafarja, M.M., Mirjalili, S., 2017. Hybrid whale optimization algorithm with simulated annealing for feature selection. Neurocomputing 260, 302–312.
Madhiarasan, M., Deepa, S.N., 2017. Comparative analysis on hidden neurons estimation in multi layer perceptron neural networks for wind speed forecasting. Artif. Intell. Rev. 48 (4), 449–471.
Marto, A., Hajihassani, M., Armaghani, D.J., Mohamad, E.T., Makhtar, A.M., 2014. A novel approach for blast-induced flyrock prediction based on imperialist competitive algorithm and artificial neural network. Sci. World J. 2014 643715. https://doi.org/10.1155/2014/643715.
Masir, R.N., Ataei, M., Mottahedi, A., 2020. Risk assessment of flyrock in surface mines using FFTA-MCDMs combination. J. Min. Environ. 12 (1), 191–203.
Mellit, A., Kalogirou, S.A., 2008. Artificial intelligence techniques for photovoltaic applications: a review. Prog. Energy Combust. Sci. 34 (5), 574–632.
Mirjalili, S., Lewis, A., 2016. The whale optimization algorithm. Adv. Eng. Software 95, 51–67.
Mirjalili, S., Mirjalili, S.M., Saremi, S., Mirjalili, S., 2020. Whale optimization algorithm: theory, literature review, and application in designing photonic crystal filters. In: Mirjalili, S., Song Dong, J., Lewis, A. (Eds.), Nature-Inspired Optimizers. Springer, pp. 219–238.
Moayedi, H., Abdullahi, M.M., Nguyen, H., Rashid, A.S.A., 2019. Comparison of dragonfly algorithm and Harris hawks optimization evolutionary data mining techniques for the assessment of bearing capacity of footings over two-layer foundation soils. Eng. Comput. 37, 437–447.
Monjezi, M., Bahrami, A., Varjani, A.Y., 2010. Simultaneous prediction of fragmentation and flyrock in blasting operation using artificial neural networks. Int. J. Rock Mech. Min. Sci. 47 (3), 476–480.

Monjezi, M., Bahrami, A., Varjani, A.Y., Sayadi, A.R., 2011. Prediction and controlling of flyrock in blasting operation using artificial neural network. Arab. J. Geosci. 4 (3–4), 421–425.
Monjezi, M., Khoshalan, H.A., Varjani, A.Y., 2012. Prediction of flyrock and backbreak in open pit blasting operation: a neuro-genetic approach. Arab. J. Geosci. 5 (3), 441–448.
Murlidhar, B.R., Kumar, D., Armaghani, D.J., Mohamad, E.T., Roy, B., Pham, B.T., 2020. A novel intelligent ELM-BBO technique for predicting distance of mine blasting-induced flyrock. Nat. Resour. Res. 29 (6), 4103–4120.
Nagano, Y., Yamaguchi, S., Fujita, Y., Koyama, M., 2019. A wrapped normal distribution on hyperbolic space for gradient-based learning. In: International Conference on Machine Learning. PLMR, pp. 4693–4702.
Nguyen, H., 2019. Support vector regression approach with different kernel functions for predicting blast-induced ground vibration: a case study in an open-pit coal mine of Vietnam. SN Appl. Sci. 1 (4), 283.
Nguyen, H., Bui, X.N., Choi, Y., Lee, C.W., Armaghani, D.J., 2020. A novel combination of whale optimization algorithm and support vector machine with different kernel functions for prediction of blasting-induced fly-rock in quarry mines. Nat. Resour. Res. 30 (1), 191–207.
Nguyen, H., Bui, X.N., Nguyen-Thoi, T., Ragam, P., Moayedi, H., 2019a. Toward a state-of-the-art of fly-rock prediction technology in open-pit mines using EANNs model. Appl. Sci. 9 (21), 1–12.
Nguyen, T., Nguyen, B.M., Nguyen, G., 2019b. Building resource auto-scaler with functional-link neural network and adaptive bacterial foraging optimization. In: Gopal, T.V., Watada, J. (Eds.), Theory and Applications of Models of Computation. Springer, pp. 501–517.
Nguyen, T., Nguyen, T., Nguyen, B.M., Nguyen, G., 2019c. Efficient time-series forecasting using neural network and opposition-based coral reefs optimization. Int. J. Comput. Intell. Syst. 12 (2), 1144–1161.
Nguyen, H., Choi, Y., Bui, X.N., Nguyen-Thoi, T., 2019d. Predicting blast-induced ground vibration in open-pit mines using vibration sensors and support vector regression-based optimization algorithms. Sensors 20 (1), 132.
Nguyen, T., Kobayashi, S., Fukuda, K., 2021. LogDTL: network log template generation with deep transfer learning. In: 2021 IFIP/IEEE International Symposium on Integrated Network Management (IM), pp. 848–853.
Nossent, J., Elsen, P., Bauwens, W., 2011. Sobol'sensitivity analysis of a complex environmental model. Environ. Model. Software 26 (12), 1515–1525.
Nourani, V., Baghanam, A.H., Adamowski, J., Kisi, O., 2014. Applications of hybrid wavelet–artificial intelligence models in hydrology: a review. J. Hydrol. 514, 358–377.
Olofsson, S.O., 1990. Applied Explosives Technology for Construction and Mining. Applex Publisher, Arla, Sweden.
Paliwal, M., Kumar, U.A., 2009. Neural networks and statistical techniques: a review of applications. Expert Syst. Appl. 36 (1), 2–17.
Rad, H.N., Hasanipanah, M., Rezaei, M., Eghlim, A.L., 2018. Developing a least squares support vector machine for estimating the blast-induced flyrock. Eng. Comput. 34 (4), 709–717.
Rahmanifard, H., Plaksina, T., 2019. Application of artificial intelligence techniques in the petroleum industry: a review. Artif. Intell. Rev. 52 (4), 2295–2318.
Raina, A.K., Murthy, V.M.S.R., 2016. Prediction of flyrock distance in open pit blasting using surface response analysis. Geotech. Geol. Eng. 34 (1), 15–28.
Raza, M.Q., Khosravi, A., 2015. A review on artificial intelligence based load demand forecasting techniques for smart grid and buildings. Renew. Sustain. Energy Rev. 50, 1352–1372.
Renzi, C., Leali, F., Cavazzuti, M., Andrisano, A.O., 2014. A review on artificial intelligence applications to the optimal design of dedicated and reconfigurable manufacturing systems. Int. J. Adv. Manuf. Technol. 72 (1–4), 403–418.
Rezaei, M., Monjezi, M., Varjani, A.Y., 2011. Development of a fuzzy model to predict flyrock in surface mining. Saf. Sci. 49 (2), 298–305.
Richards, A., Moore, A., 2004. Flyrock control–By chance or design. In: The Proceedings of the 30th Annual Conference on Explosives and Blasting Technique. The International Society of Explosives Engineers, New Orleans, Louisiana, USA, pp. 335–348.
Rosolem, R., Gupta, H.V., Shuttleworth, W.J., Zeng, X.B., De Gonçalves, L.G.G., 2012. A fully multiple-criteria implementation of the Sobol' method for parameter sensitivity analysis. J. Geophys. Res. Atmos. 117 (D7). https://doi.org/10.1029/2011JD016355.
Roy, P.P., 2005. Rock Blasting: Effects and Operations. CRC Press, Boca Raton, Florida, USA.
Salas-Rueda, R.A., 2019. Construction and evaluation of a web application for the educational process on normal distribution considering the science of data and machine learning. Res. Learn. Technol. 27, 2085.
Sheela, K.G., Deepa, S.N., 2013. Review on methods to fix number of hidden neurons in neural networks. Math. Probl Eng. 425740.
Sun, Y.J., Wang, X.L., Chen, Y.H., Liu, Z.J., 2018. A modified whale optimization algorithm for large-scale global optimization problems. Expert Syst. Appl. 114, 563–577.
Tatiya, R.R., 2005. Surface and Underground Excavations: Methods, Techniques and Equipment. A.A. Balkema, London, UK.
Tikhamarine, Y., Souag-Gamane, D., Ahmed, A.N., Sammen, S.S., Kisi, O., Huang, Y.F., El-Shafie, A., 2020. Rainfall-runoff modelling using improved machine learning methods: Harris hawks optimizer vs. particle swarm optimization. J. Hydrol. 589, 125133.
Thota, L.S., Changalasetty, S.B., 2013. Optimum learning rate for classification problem with MLP in data mining. Int. J. Adv. Eng. Technol. 6 (1), 35.
Trenn, S., 2008. Multilayer perceptrons: Approximation order and necessary number of hidden units. IEEE Trans. Neural Network. 19 (5), 836–844.
Trivedi, R., Singh, T.N., Raina, A.K., 2014. Prediction of blast-induced flyrock in Indian limestone mines using neural networks. J. Rock Mech. Geotech. Eng. 6 (5), 447–454.
Trivedi, R., Singh, T.N., Gupta, N., 2015. Prediction of blast-induced flyrock in opencast mines using ANN and ANFIS. Geotech. Geol. Eng. 33 (4), 875–891.
Trivedi, R., Singh, T., Raina, A., 2016. Simultaneous prediction of blast-induced flyrock and fragmentation in opencast limestone mines using back propagation neural network. Int. J. Min. Miner. Eng. 7 (3), 237–252.
Tuğrul, A., 2004. The effect of weathering on pore geometry and compressive strength of selected rock types from Turkey. Eng. Geol. 75 (3–4), 215–227.
Tuğrul, A., Gürpinar, O., 1997. The effect of chemical weathering on the engineering properties of Eocene basalts in northeastern Turkey. Environ. Eng. Geosci. 3 (2), 225–234.
Tuğrul, A., Zarif, I.H., 1999. Correlation of mineralogical and textural characteristics with engineering properties of selected granitic rocks from Turkey. Eng. Geol. 51 (4), 303–317.
Wan, H., Xia, J., Zhang, L.P., She, D.X., Xiao, Y., Zou, L., 2015. Sensitivity and interaction analysis based on Sobol' method and its application in a distributed flood forecasting model. Water 7 (6), 2924–2951.
Wang, L., Wu, C.Z., Tang, L.B., Zhang, W.G., Lacasse, S., Liu, H.L., Gao, L., 2020. Efficient reliability analysis of earth dam slope stability using extreme gradient boosting method. Acta Geotech 15 (11), 3135–3150.
Workman, J.L., Calder, P.N., 1994. Flyrock Prediction and Control in Surface Mine Blasting. International Society of Explosives Engineers, Cleveland, Ohio, USA.
Yi, D., Ge, X.R., 2005. An improved PSO-based ANN with simulated annealing technique. Neurocomputing 63, 527–533.
Yıldız, B.S., Yıldız, A.R., 2019. The Harris hawks optimization algorithm, salp swarm algorithm, grasshopper optimization algorithm and dragonfly algorithm for structural design optimization of vehicle components. Mater. Test. 8 (61), 60–70.
Zhang, W.G., Li, Y.Q., Wu, C.Z., Li, H.R., Goh, A.T.C., Liu, H.L., 2020a. Prediction of lining response for twin-tunnel construction in anisotropic clays using machine learning techniques. Undergr. Space. https://doi.org/10.1016/j.undsp.2020.02.007. https://doi.org/10.1016/j.undsp.2020.02.007.
Zhang, W.G., Li, H.R., Wu, C.Z., Li, Y.Q., Liu, Z.Q., Liu, H.L., 2020b. Soft computing approach for prediction of surface settlement induced by earth pressure balance shield tunneling. Undergr. Space 6 (4), 353–363.
Zhang, W.G., Li, H.R., Li, Y.Q., Liu, H.L., Chen, Y.M., Ding, X.M., 2021a. Application of deep learning algorithms in geotechnical engineering: a short critical review. Artif. Intell. Rev. https://doi.org/10.1007/s10462-021-09967-1.
Zhang, W.G., Wu, C.Z., Zhong, H.Y., Li, Y.Q., Wang, L., 2021b. Prediction of undrained shear strength using extreme gradient boosting and random forest based on Bayesian optimization. Geosci. Front. 12 (1), 469–477.
Zhang, R.H., Wu, C.Z., Goh, A.T.C., Böhlke, T., Zhang, W.G., 2021c. Estimation of diaphragm wall deflections for deep braced excavation in anisotropic clays using ensemble learning. Geosci. Front. 12 (1), 365–373.
Zhou, J., Koopialipoor, M., Murlidhar, B.R., Fatemi, S.A., Tahir, M., Armaghani, D.J., Li, C.Q., 2019. Use of intelligent methods to design effective pattern parameters of mine blasting to minimize flyrock distance. Nat. Resour. Res. 29, 625–639.
Zhou, J., Qiu, Y.G., Armaghani, D.J., Zhang, W.G., Li, C.Q., Zhu, S.L., Tarinejad, R., 2021. Predicting TBM penetration rate in hard rock condition: a comparative study among six XGB-based metaheuristic techniques. Geosci. Front. 12 (3), 101091.

Dr. Hoang Nguyen is currently working as a lecturer and researcher at the Hanoi University of Mining and Geology (HUMG), Hanoi, Vietnam. Since 2019, he has been an Assistant Professor with the Surface Mining Department, Mining Faculty, HUMG. He was a visiting researcher of Institute of Research and Development, Duy Tan University, Da Nang, Vietnam and Pukyong National University, Busan, Korea. He is the author of two books and more than 90 scientific articles. His areas of expertise include artificial intelligence, machine learning, deep learning, computer vision, optimization algorithms, metaheuristic algorithms, and advanced analytics. His domain knowledge includes advanced techniques in mining, blasting, geotechnical and geoengineering, environment, natural hazards, and natural resources research. Dr. Hoang Nguyen received the Young Talent Award in Science and Technology of HUMG in 2019.